Lukas Helfen[a,b], Thilo F. Morgeneyer[c], Feng Xu[a], Mark N. Mavrogordato[d], Ian Sinclair[d], Burkhard Schillinger[e], Tilo Baumbach[a]

[a] Institute for Synchrotron Radiation (ISS/ANKA), Karlsruhe Institute of Technology (KIT), Karlsruhe, Germany
[b] European Synchrotron Radiation Facility (ESRF), Grenoble, France
[c] Mines ParisTech, Centre des Matériaux, UMR CNRS 7633, Evry, France
[d] School of Engineering Sciences, University of Southampton, Southampton, UK
[e] FRM-II, Technische Universität München, Garching, Germany

Synchrotron and neutron laminography for three-dimensional imaging of devices and flat material specimens

Computed laminography has been introduced to synchrotron and neutron imaging set-ups to complement computed tomography for three-dimensional imaging of laterally extended (i.e. plate-like) specimens. The wide application field of computed laminography due to different contrast modes (X-ray or neutron absorption and X-ray phase contrast) and spatial resolutions ranging from some 100 down to approximately 0.5 μm is demonstrated. Selected examples from device inspection and from materials science are reported. They outline the interest of the method for non-destructive and in-situ measurements of regions of interest in large planar specimens where engineering-relevant boundary conditions have to be met. With a materials science background, the in-situ investigation of crack propagation in aluminium sheets and carbon-fibre composite panels under mechanical loading is reported.

Keywords: Laminography; Tomosynthesis; Engineering alloys; Carbon fibre composites; Damage

1. Introduction

Computed tomography (CT) is a three-dimensional (3D) imaging method well established at large scale facilities [1]. For compact or prolate specimens (i.e. long objects) extending more or less isotropically away from the rotation axis, CT is able to yield artefact-free reconstructed cross-sections. Laterally extended (i.e. flat, plate-like) specimens, however, are much less amenable to CT since reliable projection data cannot be acquired from angles where the plate is oriented parallel to the irradiation direction.

Computed laminography (CL) was introduced at synchrotron imaging set-ups [2] to overcome this limitation in specimen geometry. Despite being much less common in the materials science community, the efficiency of synchrotron-radiation CL as a method for non-destructive 3D imaging of flat, laterally extended specimens has already been demonstrated in a variety of scientific areas ranging from microsystem technology [3, 4] over cultural heritage investigations [5, 6] to paleontology [7]. Recently, a first implementation of CL with neutron radiation was reported [8] providing a sensitivity to chemical elements very different from X-rays.

Here, we present the fundamentals and the wide application field of neutron and synchrotron CL. Due to different contrast modes of X-ray and neutron attenuation or X-ray phase contrast [9, 10] and spatial resolutions ranging from about 100 down to 0.5 μm a wide research area can be addressed. Selected examples from microtechnology and materials science are reported. Some of them highlight the peculiar interest of the method for in-situ measurements of large planar specimens where engineering-relevant boundary conditions have to be met.

For example in the transportation industry, critical structures are increasingly made with laminated fibre-reinforced polymer composite materials. To reduce the time and cost associated with product development, dedicated tools for reliable damage prediction are in high demand. Also for aluminium alloys in aerospace applications the understanding of fracture mechanisms is crucial for material improvement and achievement of lighter structures leading to higher fuel efficiency [11].

In this work, the in-situ investigation of crack propagation under mechanical loading in typical engineering materials in the form of flat sheets is illustrated by examples of carbon-fibre composite panels and of aluminium plates.

2. Experimental procedure

In Fig. 1, a typical CT setup at synchrotron/neutron facilities is shown (a) and compared to the setup for CL (b).

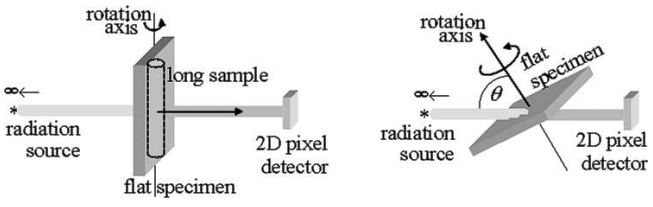

Fig. 1. Schemes of (a) a typical CT setup in comparison to the (b) CL set-up at synchrotron and neutron beamlines with parallel-beam geometry.

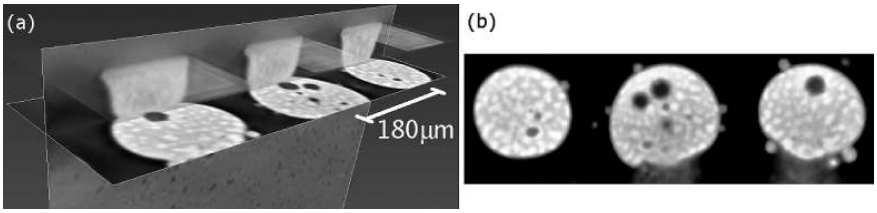

Fig. 2. (a) 3D rendering of a flip-chip bonded device with the bump bonds cut open by two perpendicular planes and also showing the underbump metallisation on the chip (top horizontal plane). (b) reconstructed cross-section through the bump bonds showing the PbSn solder microstructure and voids (voxel size 1.5 µm, 180 µm bump pitch).

Both methods rely on the acquisition of projection data of the specimen at different rotation angles and a subsequent computer-based reconstruction.

CT allows artefact-free reconstruction if the specimen does not exceed the lateral field of view of the 2D detector. For parallel-beam illumination as encountered with synchrotron or neutron imaging setups (the source usually is far from the specimen), the specimen can be elongated along the direction of the rotation axis without creating additional artefacts.

In the case of CL, the specimen is extended in two dimensions (i.e. plate-like) and a region of interest (ROI) is imaged at the crossing of beam, rotation axis and specimen. The size of this ROI depends on the field of view of the 2D detector.

Parallel-beam CT performs a complete sampling of the 3D Fourier domain of the specimen (up to a certain resolution limit) if the projection data is not truncated for any projection direction and if reliable projection data can be acquired over at least 180° rotation angle. Therefore, synchrotron CT is in principle able to yield artefact-free cross-sections for specimens which are compact or (at most) one-dimensionally elongated (see dotted sample in Fig. 1a). If the specimen is extended in two dimensions, however, the specimen attenuates almost completely the radiation for rotation angles close to parallel to the surface so that projection data are not reliable. This de facto limited-angle CT is known to lead to imaging artefacts which can be quite disturbing for the evaluation of the reconstructed cross sections [12].

Synchrotron CL on the other hand intrinsically leaves vacancies in the Fourier domain [13] which inevitably leads to imaging artefacts. Due to the better coverage of the Fourier domain (for a given maximum specimen inclination angle) and isotropic shape around the rotation axis, however, these artefacts are often less disturbing than those of limited-angle CT. For 3D image reconstruction using parallel-beam data [14], filtered backprojection is employed paying attention to preserve the sampled spatial frequencies as much as possible [13]. Parallel and distributed computation techniques [15] are used to accelerate the reconstruction process.

We performed the synchrotron experiments at ANKA's laminography instrument [16] installed at beamline ID19 of the ESRF [17], Grenoble. Neutron laminography was carried out at the ANTARES instrument [18] of the FRM-II research reactor of the Technische Universität München.

Depending on the detector resolution (i.e. on the width of the detector and its point-spread function in terms of pixels), typically 900 to 2400 projections were taken.

For the synchrotron in-situ experiments under mechanical loading, a testing rig [19, 20] was installed on the rotation stage. Anti-buckling devices were used to prevent out-of-plane torsion of the specimens under load. The mechanically loaded specimens were prepared with sizes of approximately 70×60 mm^2 and one 30 to 40 mm long notch where the cracks could initiate.

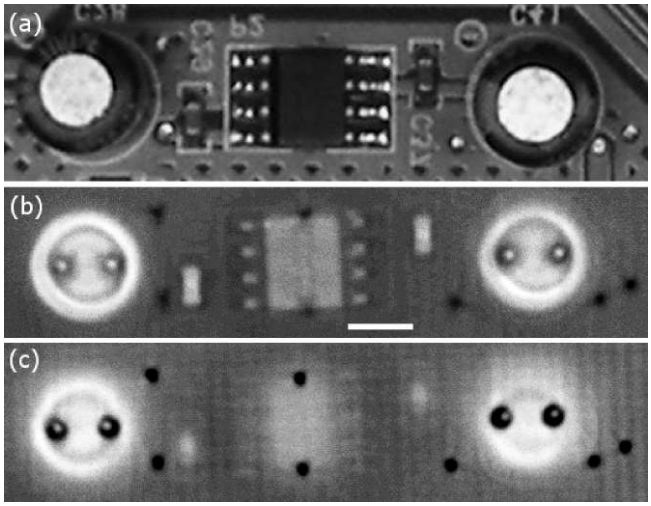

Fig. 3. (a) Optical image of a part of a printed circuit board with a packaged chip (at the centre), two surface-mounted devices and two capacitors at either side, (b) and (c) two cross-sections (300 µm apart) reconstructed by neutron laminography near the surface, i.e. through the chip packaging (b) and within the printed circuit board (c). Voxel size 58.6 µm, scale bar is 3 mm.

3. Results

Figure 2a shows a 3D rendering of three solder joints (bump bonds) of a flip-chip bonded device. The PbSn microstructure of the solder is clearly visible from the reconstructed slice (b). The voids (dark regions inside the bumps) reduce the conductive cross-section and are defects which should be avoided during the bump-bonding process.

Imaging via neutron CL of such electronic components and interconnections is illustrated in Fig. 3. Unlike X-ray imaging, attenuation of the transmitted beam is now high for the polymers contained in the printed circuit board (PCB), packaging and the capacitors. The interconnections are now weakly absorbing which can be seen in the dark spots in (c) where the capacitors' legs are soldered to the PCB.

Figure 4 shows a 3D representation of the void evolution in an AA2139 alloy sheet of data obtained via a synchrotron CL in-situ observation. Only voids and the initial notch are made visible here in a 140 µm thick slice around the sheet's central plane.

An ROI at the notch tip of a mechanically loaded carbon-fibre reinforced polymer (CFRP) specimen imaged by synchrotron laminography is shown in Fig. 5. Inside the volume one can clearly distinguish the damaged microstructure showing 0°-ply cracks as well as transverse ply cracks (TPCs).

4. Discussion

The defects in the flip-chip bump bonds identified as voids (see Fig. 2) should be avoided to ensure high reliability under electrical operation with elevated current densities and

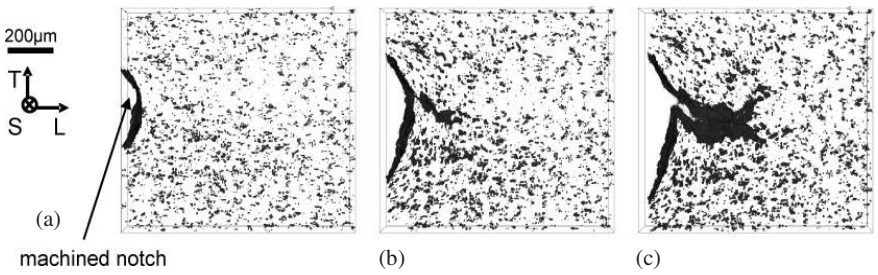

Fig. 4. Observation of void and crack evolution in an AA2 139 aluminium alloy sheet under mechanical load by synchrotron CL performed at ESRF beamline ID19 (E = 25 keV, voxel size 0.7 µm). Three different loading stages are shown as 3D renderings (140 µm thick slice around mid-thickness) only showing voids and the notch for different crack mouth opening displacements (*CMOD*) (a) at *CMOD* = 0.5 mm, (b) at *CMOD* = 1.75 mm, and (c) at *CMOD* = 2.0625 mm.

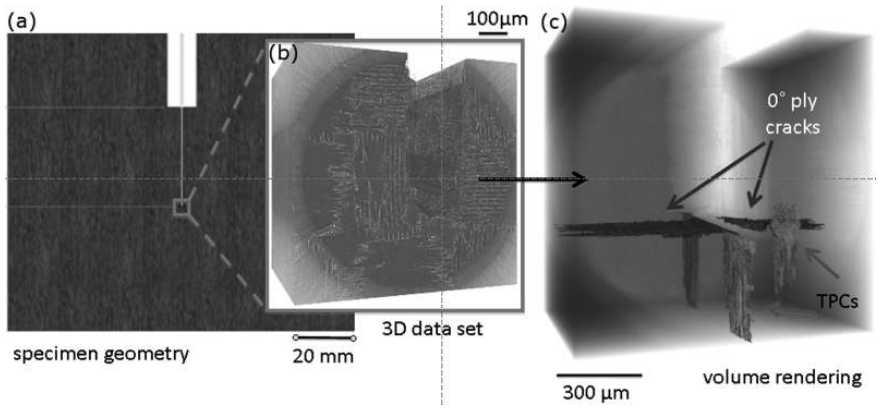

Fig. 5. Synchrotron CL measurements performed at ESRF beamline ID19 of a 4-ply carbon fibre composite panel under mechanical load (E = 20 keV, voxel size 0.7 µm). (a) sketch of the specimen geometry with notch, (b) 3D CL data set acquired showing the ROI (cylinder) at the notch tip, (c) volume rendering of the notch tip and damage in the composite panel.

thermal cycling. In-situ investigation of the voids and their evolution under current stressing enables life time predictions of such interconnections [21].

Neutron CL has just emerged as a technique [8]. Its main advantages are related to the neutron attenuation coefficients which can be very different compared to their X-ray counterparts for the different chemical elements. Spatial resolutions much better than 50 µm are difficult to obtain and may be considered as a drawback for the investigation of microstructured materials.

For engineering alloys, substantial attention has been drawn to micromechanical damage mechanisms and crack path in combination with the microstructure over the last decades [22–24]. These mechanisms have been observed via post mortem fractography assessment or via arrested cracks also involving 3D synchrotron CT [25–27]. Although damage mechanisms have been studied in-situ and in three dimensions within the material via CT [28] revealing novel insights at the micrometre scale, this technique has its limitation with respect to specimen size that is typically of the order of 1 mm in diameter for the aimed resolutions and hence does not allow one to study ductile crack initiation and propagation. The plastic zone size may be extended over several millimetres in engineering components, but also for the simple sheet geometry, which cannot be reproduced in such CT investigations. Via the CL observations described, however, these aspects and mechanisms can be studied efficiently. For example, the growth of voids between Fig. 4a and b can be seen ahead of the notch as well as the coalescence of two big voids and the notch. Voids around the notch reorient in a direction that is tangential to the notch radius. In Fig. 4c the growth of the crack can be observed with crack branching. A reduction in void growth between the initiation region and the propagation can be discerned. These data may be analysed further in terms of void growth measurement.

The damage observed for the highly anisotropic material of CFRP in Fig. 5 reveals that 0° ply splitting is occurring at the loaded notch, ameliorating the stress concentration: in this instance a toughened resin has been used, with a corresponding inhibition of delamination between plies (only 0° ply splits and TPCs are seen in this case). By visualising the incidence and extent of specific failure modes within the sample, corresponding micromechanical models are both initialised (e. g. to include certain failure modes and interactions, whilst discounting others), and calibrated (e. g. in terms of crack opening levels, length etc.), allowing for both efficient and accurate simulation tools to be developed.

5. Conclusions

As has been shown, CL opens up new possibilities in materials science and microtechnology. It has clear advantages over CT when flat specimens or material samples have to be investigated non-destructively or repeatedly. Synchrotron CL provides spatial resolutions down to just below one micrometre, and resolutions on the deep-submicron scale can be achieved via X-ray focusing [29]. Where spatial resolution is not an important criterion, neutron laminography can be a valuable alternative as it has a sensitivity towards chemical elements very different compared to the sensitivity provided by X-rays.

For microstructured materials, laminography presents vital opportunities to relate structure to true engineering behaviour, as many aspects of failure and fracture are intimately linked to the length scales of crack and overall sample geometry (e. g. in terms of elastic-plastic constraint conditions). Exploiting the non-destructive nature of X-ray imaging, it then becomes possible to visualise micromechanical processes controlling real-world performance in a time resolved, three-dimensional manner for the first time.

The help of J.-P. Valade and P. Dideron with specimen holders for the synchrotron experiments and of E. Calzada for the neutron specimen holder are acknowledged.

References

[1] Advanced Tomographic Methods in Materials Research and Engineering, J. Banhart (Ed.), Oxford University Press, New York (2008).
[2] L. Helfen T. Baumbach, P. Mikulík, D. Kiel, P. Pernot, P. Cloetens, J. Baruchel: Appl. Phys. Lett. 86 (2005) 071915.
[3] L. Helfen, A. Myagotin, P. Pernot, M. DiMichiel, P. Mikulík, A. Berthold, T. Baumbach: Nucl. Instrum. Meth. Phys. Res. A 563 (2006) 163. PMid:18097079; DOI:10.1016/j.nima.2006.01.085
[4] L. Helfen, A. Myagotin, A. Rack, P. Pernot, P. Mikulík, M. DiMichiel, T. Baumbach: Phys. Stat. Sol. A 204 (2007) 2760.
[5] K. Krug, L. Porra, P. Coan, G. Tauber, A. Wallert, J. Dik, A. Coerdt, A. Bravin, M. Elyyan, L. Helfen, T. Baumbach: J. Synchr. Rad. 15 (2008) 55. DOI:10.1107/S0909049507045438
[6] J. Dik, P. Reischig, K. Krug, A. Wallert, A. Coerdt, L. Helfen, T. Baumbach: J. Am. Inst. Conserv. 48 (2009) 185.
[7] A. Houssaye, F. Xu, L. Helfen, V. de Buffrénil, T. Baumbach, P. Tafforeau: J. Vertebr. Paleontol. 31 (2011) 2. DOI:10.1080/02724634.2011.539650
[8] L. Helfen, F. Xu, B. Schillinger, E. Calzada, I. Zanette, T. Weitkamp, T. Baumbach: Nucl. Instrum. Meth. Phys. Res. A 651 (2011) 135–139. DOI:10.1016/j.nima.2011.01.114
[9] L. Helfen, T. Baumbach, P. Cloetens, J. Baruchel: Appl. Phys. Lett. 94 (2009) 104103. DOI:10.1063/1.3089237
[10] F. Xu, L. Helfen, A.J. Moffat, G. Johnson, I. Sinclair, T. Baumbach: J. Synchr. Radiat. 17 (2010) 222. DOI:10.1107/S0909049510001512
[11] M.-V. Uz, M. Koçak, F. Lemaitre, J.-C. Ehrström, S. Kemp, F. Bron: Int. J. Fatigue 31 (2009) 916–926. DOI:10.1016/j.ijfatigue.2008.10.003
[12] L. Helfen, A. Myagotin, P. Mikulík, P. Pernot, A. Voropaev, M. Elyyan, M. DiMichiel, J. Baruchel, T. Baumbach: Rev. Sci. Instrum. 82 (2011) 063702. DOI:10.1063/1.3596566
[13] F. Xu, L. Helfen, T. Baumbach, H. Suhonen: "Comparison of image quality in computed laminography and tomography", manuscript submitted.
[14] L. Helfen, T. Baumbach, P. Pernot, P. Mikulík, M. DiMichiel, J. Baruchel: Proc. SPIE 6318 (2006), 63180N. DOI:10.1117/12.680797
[15] A. Myagotin, A. Voropaev, L. Helfen, D. Hänschke, T. Baumbach: Fast volume reconstruction for parallel-beam computed laminography by filtered backprojection, manuscript submitted.
[16] L. Helfen, V. Altapova, D. Hänschke, A. Homs Puron, J.-P. Valade, M. Nicola, M. Schneider, J. Baruchel, T. Baumbach: "ANKA's absorption and phase-contrast laminography instrument at ESRF beamline ID19", manuscript in preparation.
[17] T. Weitkamp, P. Tafforeau, E. Boller, P. Cloetens, J.-P. Valade, P. Bernard, F. Peyrin, W. Ludwig, L. Helfen, J. Baruchel: AIP Conference Proceedings 1221 (2010) 33. DOI:10.1063/1.3399253
[18] B. Schillinger, E. Calzada, K. Lorenz: Solid State Phenomena 112 (2006) 61. DOI:10.4028/www.scientific.net/SSP.112.61
[19] A.J. Moffat, P. Wright, L. Helfen, T. Baumbach, G. Johnson, S.M. Spearing, I. Sinclair: Scripta Mater. 62 (2010) 97. DOI:10.1016/j.scriptamat.2009.09.027
[20] T.F. Morgeneyer, L. Helfen, I. Sinclair, H. Proudhon, F. Xu, T. Baumbach: Scripta Mater. 65 (2011) 1010–1013. DOI:10.1016/j.scriptamat.2011.09.005
[21] T. Tian, F. Xu, J.K. Han, D. Choi, Y. Cheng, L. Helfen, M. DiMichiel, T. Baumbach, K.N. Tu: Appl. Phys. Lett. 99 (2011) 082114. DOI:10.1063/1.3628342
[22] C.Q. Chen, J.F. Knott: Met. Sci. 15 (1981) 357.
[23] D. Dumont, A. Deschamps, Y. Bréchet, C. Sigli, J.C. Ehrström: Mater. Sci. Techn. 20 (2004) 1. DOI:10.1179/026708304225016662
[24] U. Zerbst, M. Heinimann, C. Dalle Donne, D. Steglich: Eng. Frac. Mech. 76 (2009) 5. DOI:10.1016/j.engfracmech.2007.10.005
[25] T.F. Morgeneyer, M.J. Starink, I. Sinclair: Acta Mater. 56 (2008) 1671. DOI:10.1016/j.actamat.2007.12.019
[26] T.F. Morgeneyer, M.J. Starink, S.C. Wang, I. Sinclair: Acta Mater. 56 (2008) 2872. DOI:10.1016/j.actamat.2008.02.021
[27] T.F. Morgeneyer, J. Besson, H. Proudhon, M.J. Starink, I. Sinclair: Acta Mater. 57 (2009) 3902. DOI:10.1016/j.actamat.2009.04.046
[28] H. Toda, E. Maire, S. Yamauchi, H. Tsuruta, T. Hiramatsu, M. Kobayashi: Acta Mater. 59 (2011) 1995. DOI:10.1016/j.actamat.2010.11.065
[29] H. Suhonen, F. Xu, L. Helfen, C. Ferrero, P. Vladimirov, P. Cloetens: "X-ray phase contrast and fluorescence nanotomography for material studies", Int. J. Mater. Res., 103 (2012) 179. DOI:10.3139/146.110664

(Received August 1, 2011; accepted November 10, 2011)

Bibliography

DOI 10.3139/146.110668
Int. J. Mat. Res. (formerly Z. Metallkd.)
103 (2012) 2; page 170–173

ISSN 1862-5282

Correspondence address

Dr. Lukas Helfen
ISS/ANKA, Karlsruhe Institute of Technology
Herrmann-von-Helmholtz-Platz 1
D-76344 Eggenstein-Leopoldshafen, Germany
Tel.: +33 476 88 25 58
Fax: +33 476 88 22 52
E-mail: lukas.helfen@kit.edu